Acta Crystallographica Section C
Crystal Structure Communications
ISSN 0108-2701

Three 4-aminoquinolines of antimalarial interest

Susan A. Bourne,* Katherine De Villiers and Timothy J. Egan

Department of Chemistry, University of Cape Town, Rondebosch 7701, South Africa
Correspondence e-mail: xraysue@science.uct.ac.za

Received 2 November 2005
Accepted 8 December 2005
Online 14 January 2006

The structures of three compounds with potential antimalarial activity are reported. In *N*,*N*-diethyl-*N*′-(7-iodoquinolin-4-yl)ethane-1,2-diamine, $C_{15}H_{20}IN_3$, (I), the molecules are linked into ribbons by N—H···N and C—H···N hydrogen bonds. In *N*-(7-bromoquinolin-4-yl)-*N*′,*N*′-diethylethane-1,2-diamine dihydrate, $C_{15}H_{20}BrN_3\cdot 2H_2O$, (II), two aminoquinoline molecules and four water molecules form an $R_5^4(13)$ hydrogen-bonded ring which links to its neighbours to form a *T*5(2) one-dimensional infinite tape with pendant hydrogen bonds to the aminoquinolines. The phosphate salt 7-chloro-4-[2-(diethylammonio)ethylamino]quinolinium bis(dihydrogenphosphate) phosphoric acid, $C_{15}H_{22}ClN_3^{2+}\cdot 2H_2PO_4^-\cdot H_3PO_4$, (III), was prepared in order to establish the protonation sites of these compounds. The phosphate ions form a two-dimensional hydrogen-bonded sheet, while the aminoquinoline cations are linked to the phosphates by N—H···O hydrogen bonds from each of their three N atoms. While the conformation of the quinoline region hardly varies between (I), (II) and (III), the amino side chain is much more flexible and adopts a significantly different conformation in each case. Aromatic π–π stacking interactions are the only supramolecular interactions seen in all three structures.

Comment

Quinoline antimalarial drugs, such as chloroquine, quinine, amodiaquine and mefloquine, have been used as effective treatments for malaria (Tilley *et al.*, 2001). Until the onset of parasite resistance, chloroquine was especially valuable, owing to its affordability, limited toxicity and potency. It is believed to accumulate in its diprotonated state in the acidic environment of the *Plasmodium* food vacuole in an infected red blood cell, unable to re-cross the lipid membrane. The drug activity is understood to arise from complex formation between the 4-aminoquinoline drug and its target, haematin, thus preventing the haematin from aggregating to crystalline haemozoin (Egan *et al.*, 1994). The structure–activity relationships for a series of aminoquinolines have been investigated in order to determine which molecular constituents confer antimalarial activity (Kaschula *et al.*, 2002). A 4-aminoquinoline nucleus provides a planar electron-rich conjugated system able to associate with the porphyrin dimer. A moderately electron-withdrawing and strongly lipophilic group at position 7 is needed to maximize the drug activity, while the terminal amino group is basic and helps to ensure that the drug accumulates in the acidic food vacuole.

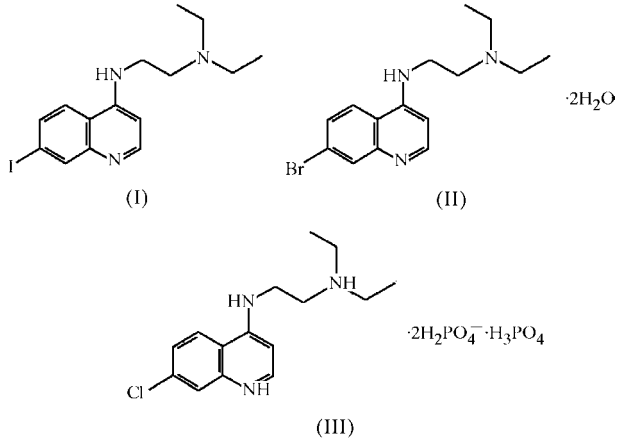

Molecular modelling provides a useful probe for investigating these complexes and crystallographic studies can provide complementary information about the structure of 4-aminoquinoline compounds. As part of an ongoing study into the mechanism of antimalarial drug activity, we have elucidated the crystal structures of three short-chain 4-aminoquinolines, *viz.* *N*,*N*-diethyl-*N*′-(7-iodoquinolin-4-yl)-ethane-1,2-diamine, (I), *N*-(7-bromoquinolin-4-yl)-*N*′,*N*′-diethylethane-1,2-diamine dihydrate, (II), and 7-chloro-4-[2-(diethylammonio)ethylamino]quinolinium bis(dihydrogenphosphate) phosphoric acid, (III) (see scheme). This class of compounds has been shown to inhibit the formation of synthetic β-haematin and to exhibit antiplasmodial activity *in vitro* (Kaschula *et al.*, 2002), and they are therefore potential

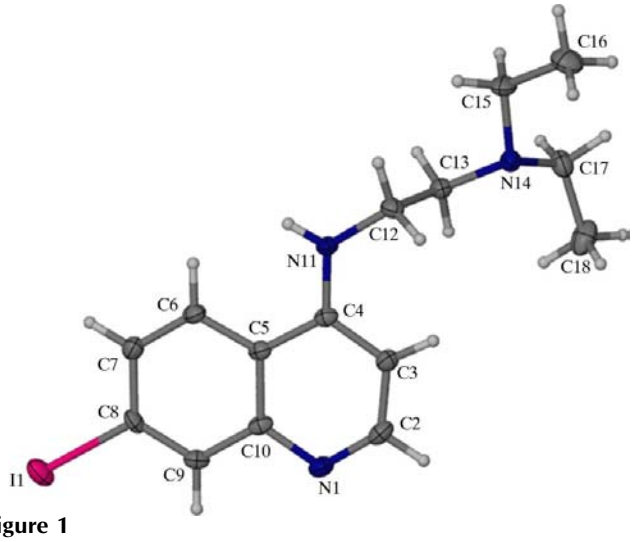

Figure 1
The molecule of (I), showing the atom-labelling scheme. Displacement ellipsoids are drawn at the 50% probability level and H atoms are shown as small spheres of arbitrary radii.

 DOI: 10.1107/S0108270105041235

antimalarials. While this class of compounds forms complexes with haematin and prevents its aggregation to crystalline haemozoin, complexes between the drug molecule and haematin are notoriously difficult to crystallize. Molecular modelling using computational methods may provide a means of studying such interactions in solution.

The crystal structures obtained in this study are valuable for comparison with the structures generated using molecular modelling. The intermolecular parameters determined from the crystal structures were compared with those of related compounds generated using molecular modelling. The results of these computational investigations will be reported separately.

The iodo compound, (I), is shown in Fig. 1. The bromoquinoline derivative crystallizes with two water molecules to form (II) (Fig. 2). The asymmetric unit of (III) consists of two crystallographically independent quinoline molecules (labelled *A* and *B*), and six phosphate ions (Fig. 3); structural refinement confirmed that the diprotic salt of *N*′-(7-chloroquinolin-4-yl)-*N*,*N*-diethyl-1,2-ethanediamine had crystallized.

The molecular conformations of compounds (I)–(III) can be defined in terms of six torsion angles, which are given in Table 1. The quinoline rings are planar in each case. Thus, the only conformational differences arise within the diamine side chain. The N11—C12 bond is nearly coplanar with the ring system in each case, with the greatest deviation being in molecule *A* of (III). The torsion angles C4—N11—C12—C13 (τ_2) and N11—C12—C13—N14 (τ_3) show that for (I), the side chain is in the more extended conformation induced by the *gauche* and *anti* conformations in τ_2 and τ_3, respectively. In (II), these torsion angles are *anti* and *gauche*, while in (III) they are both *gauche*, in each case resulting in the side chain folding back to a greater degree. The three different side chain conformations are shown in Fig. 4. NMR-constrained molecular mechanics and molecular dynamics/simulated annealing studies (Leed *et al.*, 2002) have found that, on complexation with haematin, the aliphatic side chains of chloroquine, quinine and quinidine fold back to interact with the tetrapyrrole. It should be noted that the more extended conformation observed in this study may therefore change significantly on complexation.

In the supramolecular structure of (I), quinoline atom N1 of the molecule at (*x*, *y*, *z*) acts as a hydrogen-bond acceptor to

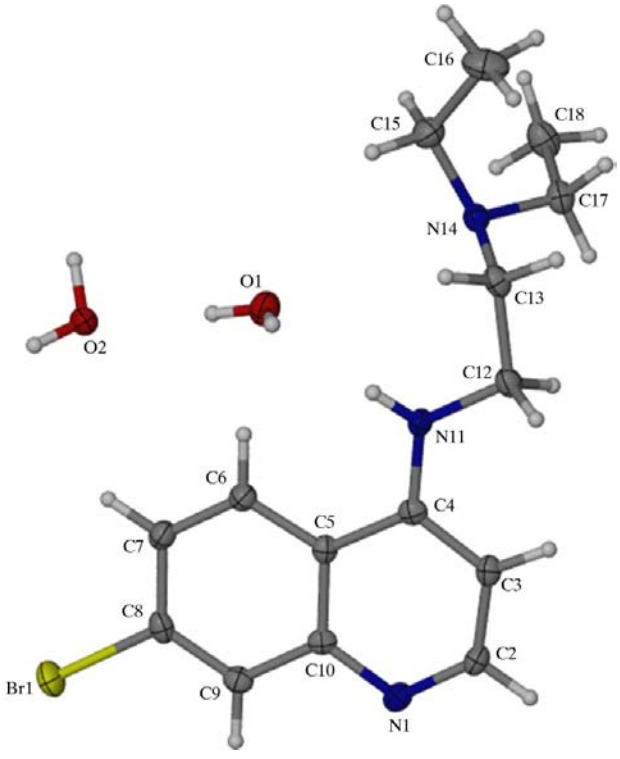

Figure 2
The asymmetric unit of (II), showing the atom-labelling scheme. Displacement ellipsoids are drawn at the 50% probability level and H atoms are shown as small spheres of arbitrary radii.

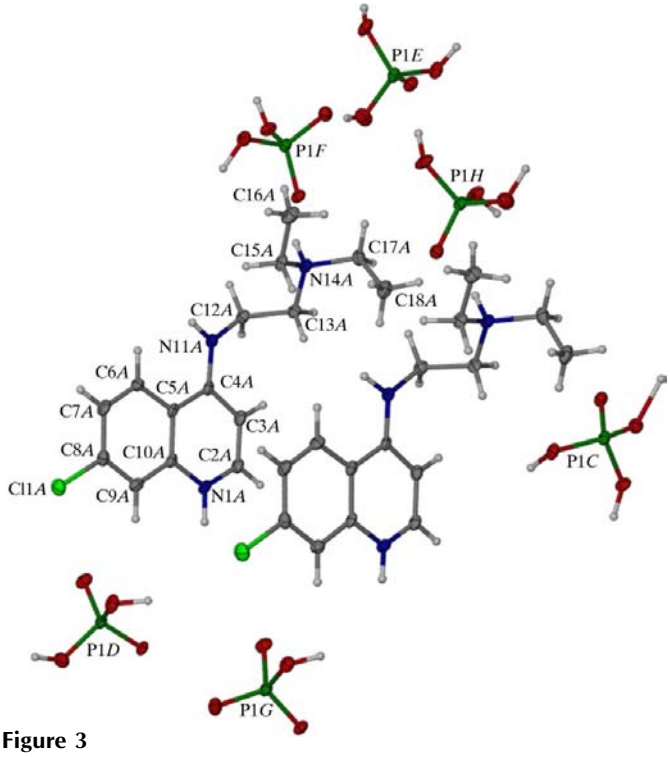

Figure 3
The asymmetric unit of (III), showing the atom-labelling scheme for molecule *A*; molecule *B* is similarly numbered. Displacement ellipsoids are drawn at the 50% probability level and H atoms are shown as small spheres of arbitrary radii.

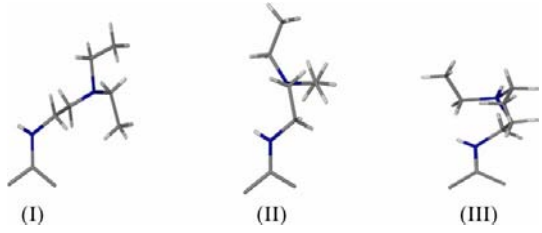

Figure 4
The conformations of the diamine side chain in compounds (I), (II) and (II). For (III), molecule *A* is illustrated; the side chain of molecule *B* has an almost identical conformation.

the 4-amino group (atom N11) and quinoline atom C6 of the molecule at $(\frac{1}{2}+x, y, \frac{1}{2}-z)$, generating an $R_2^1(7)$ ring (Table 2) (Bernstein *et al.*, 1995). Propagation by a twofold screw axis generates a ribbon of molecules parallel to [100] (Fig. 5). Perpendicular to the ribbons, molecules stack in parallel orientations to allow π–π interactions between adjacent quinoline rings (centroid separations are between 3.82 and 4.53 Å).

Intermolecular hydrogen bonds are prominent in the crystal structure of (II) (Table 3). Two aminoquinoline molecules and four water molecules form an $R_5^4(13)$ hydrogen-bonded ring. These rings then form a linked network with shared O1—H···O2 edges. This network is illustrated in Fig. 6 as dashed lines. O2—H22*W*···N1(quinoline) hydrogen-bonded chains (shown as thin solid lines in Fig. 6) are pendant to these rings. It is worth noting that this arrangement allows each aminoquinoline N atom to act as either a hydrogen-bond acceptor (N1 and N14) or donor (N11). Water is potentially capable of participating in four hydrogen bonds but frequently shows a three-coordinate configuration (Jeffrey & Maluszynska, 1990). This is illustrated in the case of (II), where atom O1 donates two hydrogen bonds but accepts one, while atom O2 participates in a full quota of four hydrogen bonds. Infantes *et al.* (2002, 2003) have investigated the role of water molecules in stabilizing hydrated crystal structures of organic compounds. The hydrogen-bonded rings in (II) form the relatively common one-dimensional infinite tapes denoted by Infantes as *T*5(2). Aromatic stacking is again significant in this structure (centroid separations of 3.57 and 3.58 Å). In addition, a Br···Br interaction [distance = 3.6967 (5) Å; sum of radii = 3.70 Å (Desiraju, 1989)] is also evident.

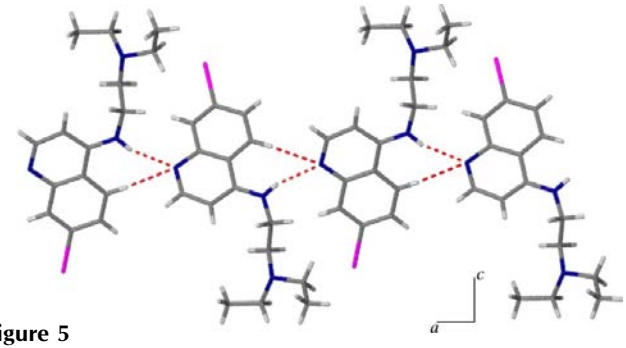

Figure 5
Part of the crystal structure of (I), showing the formation of a ribbon of $R_2^1(7)$ rings along [100].

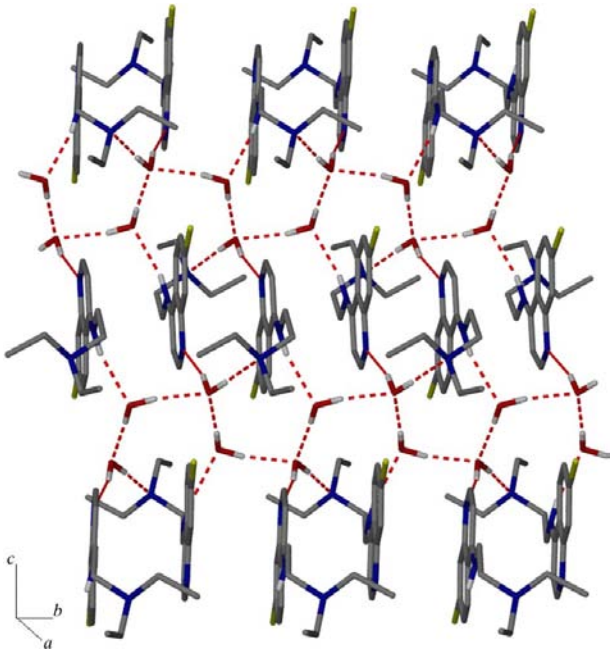

Figure 6
A packing diagram for compound (II), indicating the linked $R_5^4(13)$ rings (dashed lines) and appended O2···N1 chains (thin solid lines). H atoms not involved in the hydrogen bonding have been omitted for clarity.

The phosphate salt (III) was prepared in order to confirm that protonation of these compounds occurs at the terminal amine and quinoline N atoms. The conformations of aminoquinoline molecules *A* and *B* are essentially identical but there are six crystallographically independent phosphate ions in the asymmetric unit. As in (I) and (II), there is an extended network of hydrogen bonds stabilizing the structure. A list of 'strong' hydrogen bonds is given in Table 4; there are also a large number of C—H···O interactions, but these have not been detailed. Aromatic stacking also plays a role in the crystal packing, which takes the form of stacks of aminoquinoline and phosphate ions. The phosphate ions form a two-dimensional hydrogen-bonded sheet parallel to $[\bar{1}11]$, similar to those reported for anilinium phosphate salts (Paixão *et al.*, 2000; Mahmoudkhani & Langer, 2002). We note that all hydrogen bonds within this sheet are of the form P—O—H···O=P, with correspondingly short O···O distances (2.48–2.67 Å). This phenomenon has been noted previously: shorter bonds (*ca* 2.5 Å) connect P—O—H and P=O groups, while longer distances (*ca* 2.8 Å) link P—O—H moieties on adjacent molecules (Greenwood & Earnshaw, 1984; Dega-Szafran *et al.*, 2000). In addition, P—O bond lengths corroborate the assignment of P—O—H (between 1.53 and 1.58 Å) and P=O bonds (between 1.49 and 1.52 Å) within the phosphates. Aminoquinoline cations are linked to the phosphate anions

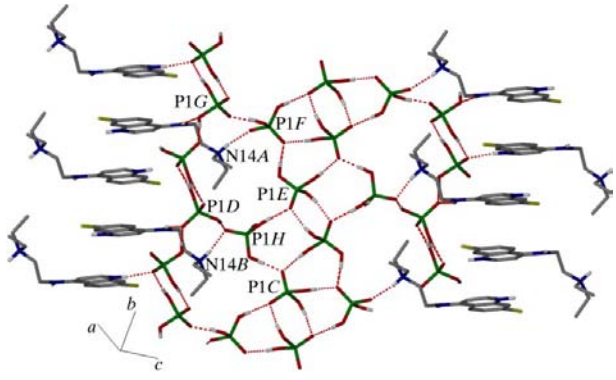

Figure 7
Part of the crystal structure of (III), showing the formation of a two-dimensional hydrogen-bonded sheet of phosphate ions and aminoquinoline stacks. H atoms not involved in the hydrogen bonding have been omitted for clarity.

via N—H···O—P hydrogen bonds. The aromatic ends of the quinolines point towards the phosphate layer and stack with their Cl atoms in alternating directions (centroid separations are in the range 3.65–3.95 Å). These features are illustrated in Fig. 7.

In conclusion, the molecular constituents of (I)–(III) potentially allow four different types of direction-specific intermolecular interactions. These are N—H···N and C—H···N hydrogen bonds, halogen interactions and aromatic π–π stacking interactions. In fact, the only interaction observed in all three structures is the last of these. In (I), N—H···N and C—H···N hydrogen bonds govern the supramolecular network, while in (II) and (III) the stronger hydrogen-bonding capability of O atoms (in water molecules or phosphate ions) dominates. The molecular conformation of the quinoline nucleus hardly varies between the three structures, while the amino side chain is found to be much more flexible. The conformations of these three related 7-haloaminoquinolines and the patterns in their supramolecular networks suggest there is a subtle interplay between the weak direction-specific interactions between molecules. Weak forces of the type seen here, which depend on molecular polarizability, are not easy to model computationally, especially in the prediction of supramolecular structures. The variation in the supramolecular aggregation observed in these compounds suggests that experimental results of the type reported here are likely to be of prime importance for some time to come.

The observation of the two protonation sites in (III) is important. The terminal amine N atom has been previously recognized as a site of protonation but some uncertainty existed as to whether the second protonation site is the 4-amino or the quinoline N atom. This study provides evidence that the second protonation site is indeed the latter.

Experimental

Compounds (I)–(III) were synthesized for an earlier study by reaction of *N*,*N*-diethylethane-1,2-diamine with the corresponding 7-substituted 4-chloroquinolines (Kaschula *et al.*, 2002). Single crystals of the free base forms of (I) and (II) were obtained by dissolving the respective compounds (*ca* 12 mg) in a minimum volume of diethyl ether and allowing slow evaporation of the solvent in a refrigerator (283 K). Compound (III) (*ca* 10 mg) was dissolved in a dilute solution of phosphoric acid to facilitate the formation of the diprotic species. An aliquot of *n*-hexane was added to the solution and the vial placed in a refrigerator (283 K) to allow slow mixing of the solvent layers. Needle-like crystals formed in the aqueous layer within one week.

Table 1
Selected torsion angles (°).

τ_1 = C3—C4—N11—C12, τ_2 = C4—N11—C12—C13, τ_3 = N11—C12—C13—N14, τ_4 = C12—C13—N14—C15, τ_5 = C13—N14—C15—C16 and τ_6 = C13—N14—C17—C18.

Compound	τ_1	τ_2	τ_3	τ_4	τ_5	τ_6
(I)	−2.8 (2)	80.6 (4)	−171.2 (2)	−74.8 (3)	160.6 (3)	−69.9 (4)
(II)	−2.6 (3)	−177.2 (2)	−70.9 (3)	156.2 (2)	67.9 (3)	176.5 (2)
(III*A*)	8.6 (3)	−81.5 (4)	−91.3 (3)	64.1 (3)	−177.0 (3)	−74.2 (3)
(III*B*)	2.4 (2)	78.0 (4)	91.2 (3)	62.5 (3)	178.9 (2)	71.1 (3)

Compound (I)

Crystal data

$C_{15}H_{20}IN_3$
M_r = 369.24
Orthorhombic, *Pbca*
a = 13.2379 (7) Å
b = 7.8883 (4) Å
c = 29.4118 (17) Å
V = 3071.3 (3) Å^3
Z = 8
D_x = 1.597 Mg m^{-3}
Mo *K*α radiation
Cell parameters from 9238 reflections
θ = 3.1–27.2°
μ = 2.08 mm^{-1}
T = 114 (2) K
Plate, pale yellow
0.10 × 0.10 × 0.02 mm

Data collection

Nonius KappaCCD area-detector diffractometer
ω and φ scans
Absorption correction: multi-scan (*SADABS*; Sheldrick, 2000)
T_{min} = 0.820, T_{max} = 0.961
34000 measured reflections
3328 independent reflections
2401 reflections with $I > 2\sigma(I)$
R_{int} = 0.053
θ_{max} = 27.2°
h = −16 → 16
k = −9 → 10
l = −37 → 37

Refinement

Refinement on F^2
$R[F^2 > 2\sigma(F^2)]$ = 0.036
$wR(F^2)$ = 0.081
S = 1.05
3328 reflections
178 parameters
H atom: see below
$w = 1/[\sigma^2(F_o^2) + (0.0361P)^2 + 3.0942P]$ where $P = (F_o^2 + 2F_c^2)/3$
$(\Delta/\sigma)_{max}$ = 0.001
$\Delta\rho_{max}$ = 1.14 e Å^{-3}
$\Delta\rho_{min}$ = −1.02 e Å^{-3}

Table 2
Hydrogen-bond geometry (Å, °) for (I).

D—H···*A*	*D*—H	H···*A*	*D*···*A*	*D*—H···*A*
N11—H11···N1^{i}	0.83 (3)	2.22 (3)	3.019 (4)	161 (3)
C6—H6···N1^{i}	0.95	2.59	3.504 (4)	163

Symmetry code: (i) $x - \frac{1}{2}, y, -z + \frac{1}{2}$.

Compound (II)

Crystal data

$C_{15}H_{20}BrN_3 \cdot 2H_2O$
M_r = 358.28
Monoclinic, *C*2/*c*
a = 28.0177 (4) Å
b = 6.8221 (9) Å
c = 18.9339 (4) Å
β = 113.61 (3)°
V = 3316.1 (9) Å^3
Z = 8
D_x = 1.435 Mg m^{-3}
Mo *K*α radiation
Cell parameters from 8774 reflections
θ = 1.6–26.4°
μ = 2.49 mm^{-1}
T = 113 (2) K
Plate, colourless
0.13 × 0.10 × 0.10 mm

Data collection

Nonius KappaCCD area-detector diffractometer
ω and φ scans
Absorption correction: multi-scan (*SADABS*; Sheldrick, 2000)
T_{min} = 0.738, T_{max} = 0.789
26586 measured reflections
3403 independent reflections
2470 reflections with $I > 2\sigma(I)$
R_{int} = 0.074
θ_{max} = 26.4°
h = −34 → 34
k = −8 → 8
l = −23 → 23

Refinement

Refinement on F^2
$R[F^2 > 2\sigma(F^2)]$ = 0.037
$wR(F^2)$ = 0.080
S = 1.04
3403 reflections
212 parameters
H atom: see below
$w = 1/[\sigma^2(F_o^2) + (0.0305P)^2 + 3.5408P]$ where $P = (F_o^2 + 2F_c^2)/3$
$(\Delta/\sigma)_{max}$ = 0.002
$\Delta\rho_{max}$ = 0.38 e Å^{-3}
$\Delta\rho_{min}$ = −0.51 e Å^{-3}

Table 3
Hydrogen-bond geometry (Å, °) for (II).

D—H···A	D—H	H···A	D···A	D—H···A
N11—H11···O1	0.84 (2)	2.22 (3)	3.038 (3)	166 (3)
O1—H11W···O2^{i}	0.93 (3)	2.01 (3)	2.924 (3)	169 (3)
O1—H12W···O2	0.79 (3)	2.03 (3)	2.824 (3)	176 (3)
O2—H22W···N1^{ii}	0.88 (3)	1.86 (3)	2.722 (3)	166 (3)
O2—H21W···N14^{i}	0.84 (3)	2.14 (3)	2.977 (3)	172 (3)

Symmetry codes: (i) $-x+\frac{1}{2}, y+\frac{1}{2}, -z+\frac{1}{2}$; (ii) $x, -y+2, z-\frac{1}{2}$.

Compound (III)

Crystal data

$C_{15}H_{22}ClN_3^{2+}\cdot 2H_2O_4P^-\cdot H_3O_4P$	$Z = 4$
$M_r = 571.77$	$D_x = 1.643$ Mg m^{-3}
Triclinic, $P\overline{1}$	Mo $K\alpha$ radiation
$a = 11.0960$ (2) Å	Cell parameters from 9976 reflections
$b = 14.6481$ (3) Å	$\theta = 1.5$–$26.8°$
$c = 15.1797$ (4) Å	$\mu = 0.44$ mm^{-1}
$\alpha = 79.5520$ (10)°	$T = 113$ (2) K
$\beta = 88.0190$ (10)°	Plate, colourless
$\gamma = 72.3360$ (10)°	0.25 × 0.15 × 0.04 mm
$V = 2311.38$ (9) Å^3	

Data collection

Nonius KappaCCD area-detector diffractometer	9766 independent reflections
ω and φ scans	6450 reflections with $I > 2\sigma(I)$
Absorption correction: multi-scan (*SADABS*; Sheldrick, 2000)	$R_{int} = 0.128$
$T_{min} = 0.898$, $T_{max} = 0.984$	$\theta_{max} = 26.8°$
42956 measured reflections	$h = -14 \rightarrow 13$
	$k = -18 \rightarrow 18$
	$l = -19 \rightarrow 19$

Refinement

Refinement on F^2	H atoms treated by a mixture of independent and constrained refinement
$R[F^2 > 2\sigma(F^2)] = 0.054$	$w = 1/[\sigma^2(F_o^2) + (0.0549P)^2]$ where $P = (F_o^2 + 2F_c^2)/3$
$wR(F^2) = 0.140$	$(\Delta/\sigma)_{max} = 0.001$
$S = 1.00$	$\Delta\rho_{max} = 0.54$ e Å^{-3}
9766 reflections	$\Delta\rho_{min} = -0.75$ e Å^{-3}
697 parameters	

H atoms attached to N or O atoms were located in difference maps and included in the refinements with independent displacement parameters. All other H atoms were placed in geometrically calculated positions and refined as riding atoms, with C—H = 0.95–0.99 Å and U_{iso}(H) = 1.2U_{eq}(C), or 1.5U_{eq}(C) for methyl groups. Since there are only four protonation sites on the two quinoline molecules in (III), it seems reasonable to surmise that four of the six phosphates exist as $H_2PO_4^-$, each having donated one proton. In dilute aqueous solution, phosphoric acid behaves as a strong acid but only one of its H atoms is readily ionizable. The pK_a values are 2.15, 7.20 and 12.37 for the successive loss of protons (Weast, 1974). The remaining two phosphates are most likely in the form H_3PO_4, and the location of the H atoms in the difference Fourier map seemed to confirm this.

For all compounds, data collection: *COLLECT* (Nonius, 1997); cell refinement: *DENZO* (Otwinowski & Minor, 1997); data reduction: *DENZO*; program(s) used to solve structure: *SHELXS97* (Sheldrick, 1997); program(s) used to refine structure: *SHELXL97* (Sheldrick, 1997); molecular graphics: *POV-Ray* (Cason, 2003); software used to prepare material for publication: *SHELXL97* and *PLATON* (Spek, 2003).

Table 4
Hydrogen-bond geometry (Å, °) for (III).

D—H···A	D—H	H···A	D···A	D—H···A
N1A—H1A···O5D^{i}	0.98 (3)	1.81 (3)	2.787 (3)	171 (3)
N11A—H11B···O3G	0.90 (4)	2.14 (4)	3.026 (3)	167 (4)
N14A—H14A···O2F	0.87 (3)	1.95 (3)	2.777 (3)	158 (3)
N1B—H1B···O5G^{ii}	0.90 (3)	1.85 (3)	2.742 (3)	169 (3)
N11B—H11A···O3D	0.99 (4)	1.97 (4)	2.908 (3)	158 (3)
N14B—H14B···O4H	0.95 (3)	1.82 (3)	2.747 (3)	165 (3)
O4C—H4C···O3F^{iii}	1.01 (3)	1.56 (3)	2.563 (3)	176 (4)
O5C—H5C···O2C^{iv}	0.99 (3)	1.69 (4)	2.672 (3)	168 (4)
O2D—H2D···O5D^{v}	1.02 (4)	1.53 (4)	2.536 (3)	167 (5)
O4D—H4D···O4H	0.92 (4)	1.71 (4)	2.625 (3)	172 (6)
O2E—H2E···O3F	1.00 (4)	1.49 (4)	2.491 (3)	174 (5)
O3E—H3E···O4E^{iii}	0.92 (3)	1.69 (3)	2.601 (3)	169 (4)
O5E—H5E···O3C^{iii}	0.88 (3)	1.66 (3)	2.544 (3)	173 (4)
O4F—H4F···O4G	1.04 (3)	1.45 (3)	2.483 (3)	171 (3)
O5F—H5F···O2C^{vi}	0.88 (3)	1.74 (3)	2.625 (3)	177 (4)
O2G—H2G···O5G^{vii}	0.94 (3)	1.65 (4)	2.582 (3)	172 (5)
O3G—H3G···O3D^{v}	0.90 (3)	1.63 (3)	2.535 (3)	175 (4)
O2H—H2H···O4E	0.97 (3)	1.56 (3)	2.528 (3)	173 (4)
O3H—H3H···O3C	1.04 (3)	1.47 (3)	2.506 (3)	176 (4)
O5H—H5H···O2F^{viii}	0.93 (4)	1.57 (4)	2.501 (3)	176 (6)

Symmetry codes: (i) $x+1, y, z$; (ii) $x+1, y-1, z$; (iii) $-x, -y+1, -z+2$; (iv) $-x, -y, -z+2$; (v) $-x+1, -y+1, -z+1$; (vi) $x, y+1, z$; (vii) $-x+1, -y+2, -z+1$; (viii) $-x+1, -y+1, -z+2$.

Supplementary data for this paper are available from the IUCr electronic archives (Reference: HJ1079). Services for accessing these data are described at the back of the journal.

References

Bernstein, J., Davis, R. E., Shimoni, L. & Chang, N.-L. (1995). *Angew. Chem. Int. Ed. Engl.* **34**, 1555–1573.
Cason, C. J. (2003). *POV-Ray for Windows*. Version 3.1. Persistence of Vision Raytracer Pty. Ltd., Victoria, Australia. URL: http://www.povray.org/
Dega-Szafran, Z., Gzella, A., Kosturkiewicz, Z., Szafran, M. & Antkowiak, A. (2000). *J. Mol. Struct.* **555**, 67–74.
Desiraju, G. R. (1989). *Crystal Engineering: The Design of Organic Solids*. Amsterdam: Elsevier.
Egan, T. J., Ross, D. C. & Adams, P. A. (1994). *FEBS Lett.* **352**, 54–57.
Greenwood, N. N. & Earnshaw, A. (1984). *Chemistry of the Elements*, pp. 54, 585–599. Oxford: Pergamon Press.
Infantes, L., Chisholm, J. & Motherwell, S. (2003). *CrystEngComm*, **5**, 480–486.
Infantes, L. & Motherwell, S. (2002). *CrystEngComm*, **4**, 454–461.
Jeffrey, G. A. & Maluszynska, H. (1990). *Acta Cryst.* B**46**, 546–549.
Kaschula, C. H., Egan, T. J., Hunter, R., Basilico, N., Parapini, S., Taramelli, D., Pasini, E. & Monti, D. (2002). *J. Med. Chem.* **45**, 3531–3539.
Leed, A., DuBay, K., Ursos, L. M. B., Sears, D., de Dios, A. C. & Roepe, P. D. (2002). *Biochemistry*, **41**, 10245–10255.
Mahmoudkhani, A. H. & Langer, V. (2002). *J. Mol. Struct.* **609**, 55–60.
Nonius (1997). *KappaCCD Server Software*. Windows 3.11 Version. Nonius BV, Delft, The Netherlands.
Otwinowski, Z. & Minor, W. (1997). *Methods in Enzymology*, Vol. 276, *Macromolecular Crystallography*, Part A, edited by C. W. Carter Jr & R. M. Sweet, pp. 307–326. New York: Academic Press.
Paixão, J. A., Matos Beja, A., Ramos Silva, M. & Martin-Gil, J. (2000). *Acta Cryst.* C**56**, 1132–1135.
Sheldrick, G. M. (1997). *SHELXS97* and *SHELXL97*. University of Göttingen, Germany.
Sheldrick, G. M. (2000). *SADABS*. University of Göttingen, Germany.
Spek, A. L. (2003). *J. Appl. Cryst.* **36**, 7–13.
Tilley, L., Loria, P. & Foley, M. (2001). *Antimalarial Chemotherapy: Mechanisms of Action, Resistance and New Directions in Drug Discovery*, edited by P. J. Rosenthal, pp. 87–121. New Jersey: Humana Press.
Weast, R. C. (1974). Editor. *CRC Handbook of Chemistry and Physics*, p. D-130. Cleveland: CRC Press Inc.